

Dynamics of aerosol generation and flow during inhalation for improved *in vitro*–*in vivo* correlation (IVIVC) of pulmonary medicines

Agata Dorosz*^{ID}, Arkadiusz Moskal^{ID}, Tomasz R. Sosnowski^{ID}

Warsaw University of Technology, Faculty of Chemical and Process Engineering, Waryńskiego 1, 00-645 Warsaw, Poland

* Corresponding author:

e-mail:
agata.dorosz@pw.edu.pl

Article info:

Received: 16 May 2023
Revised: 16 July 2023
Accepted: 04 September 2023

Abstract

Chemical and process engineering offers scientific tools for solving problems in the biomedical field, including drug delivery systems. This paper presents examples of analyzing the dynamics of dispersed systems (aerosols) in medical inhalers to establish a better relationship between the test evaluation results of these devices and the actual delivery of drugs to the lungs. This relationship is referred to as *in vitro*–*in vivo* correlation (IVIVC). It has been shown that in dry powder inhalers (DPIs), the aerosolization process and drug release times are determined by the inhalation profile produced by the patient. It has also been shown that inspiratory flow affects the size distribution of aerosols generated in other inhalation devices (vibrating mesh nebulizers, VMNs), which is due to the evaporation of droplets after the aerosol is mixed with additional air taken in by the patient. The effects demonstrated in this work are overlooked in standard inhaler testing methods, leading to inaccurate information about the health benefits of aerosol therapy, thus limiting the development of improved drug delivery systems.

Keywords

aerosol dynamics, inhalation, resuspension, nebulization, drug delivery systems

1. INTRODUCTION

Chemical engineering finds its valuable applications in biomedical field, e.g., by offering the possibility of deeper physical analysis into the functioning of drug delivery systems. One of such systems are medical inhalers, where aerosols are used as convenient carriers for targeted drug delivery to the lower respiratory tract (Sosnowski, 2023).

The process of aerosol generation can proceed in different ways depending on the properties of the precursor. Powders are dispersed by aerodynamic forces, typically generated by the flow of inhaled air in so-called passive dry powder inhalers (DPIs) (Azouza and Chrystyn, 2012; Dorosz et al., 2021; Longest et al., 2013). Liquid solutions or suspensions are dispersed by atomization done with various methods, with pneumatic or ultrasonic nebulization (including vibrating mesh nebulization) being the most common (Sosnowski et al., 2021). In any aerosol generation system, the mass output and size distribution of dispersed particles or droplets are influenced by aerodynamic conditions of airflow through the inhaler (Dorosz et al. 2021; Sosnowski, 2016). By affecting the aerosol size distribution, these conditions determine the penetration and deposition of the drug inside the respiratory system, and thus – the effectiveness of inhalation therapies. Regardless of the type of inhaler, the actual behavior of the aerosol particles in the surrounding airflow field in the respiratory tree depends on the way of the inhalation maneuver.

Successful application of *in vitro* aerosol studies in the respiratory drug delivery applications relies on proper consider-

ation of the actual (*in vivo*) regional deposition of inhaled particles in the lungs. This has far-reaching benefits for pulmonary specialists, drug developers and, most importantly, patients. This relationship is known as *in vitro* – *in vivo* correlation (IVIVC) and is often studied in conjunction with Quality by Design (QbD) approaches (Newman and Chan, 2008, 2020; Buttini et al., 2018). Compendial recommendations require the use of cascade impactors, such as Andersen or NGI (Next Generation Impactor), to assess *in vitro* aerosol quality during product development and regular quality assessment in production (EDQM, 2021; United States Pharmacopeial Convention, 2021). The historical IVIVC studies have shown that realistic *in vivo* conditions were difficult to achieve due to technical limitations. These included e.g., unrealistic inhalation parameters (constant instead of the realistic time-varying airflow), neglecting inter-subject variability in respiratory geometry (especially – in the oropharyngeal region), but also lack of liquid coating of the surface of the impactor inlet resulting in particle rebound (Newman and Chan, 2020). It shows that standard methods for testing inhalers and medical aerosols lack the appropriate physical analysis necessary to fully understand particle dynamics. Some of these issues have been addressed (for DPI, e. g. Colthorpe et al. (2013); Delvadia et al. (2012 and 2013); Newman and Chan (2020); Wei et al. (2017, 2018) and for nebulizers e. g. Corcoran et al. (2003); Hatley and Byrne (2017); Svensson et al. (2018)). Additional research opportunities are provided with novel experimental methods. Laser diffraction (LD) is a technique that allows detailed and dynamic measurements of polydisperse aerosols with uni- or multimodal size distributions, such



as these produced from pharmaceutical formulations (Marriott et al. 2006; Shekunov et al. 2007; Telko and Hickey, 2005). Unfortunately, this optical technique does not distinguish the particles of the active pharmaceutical ingredient from the carrier (lactose) typically present in powder formulations, and thus it is not a standard method in the quality assessment of medical aerosols formed from powders. Nevertheless, in the fundamental research, LD allows analysis of time-dependent disintegration process of powders with the subsequent flow of smaller aggregates and primary particles of different sizes. Aerosolization of powders in dry powder inhalers (DPIs) proceeds in several stages: (1) fluidization of the powder bed (mechanically by impaction and aerodynamically by shear forces), (2) resuspension, and (3) deaggregation (Gac et al., 2008). The final particle size distribution (PSD) determines the behavior of aerosol particles after inhalation into the respiratory system, and it also defines their settlement mechanisms (impaction, sedimentation, Brownian diffusion) allowing to predict regional drug deposition in the lungs. The fate of each individual aerosol particle is determined by elementary phenomena such as the timing of its formation (e.g., release from the powder structure) and flow dynamics in the inhaler and human respiratory system. The cumulative effect of these phenomena in the entire particle population determines the total drug dose delivered to the desired site of action in the lungs. Therefore, studies of this type are useful in gathering comprehensive knowledge of the course of fine drug particles release from the surface of larger aggregates or carrier grains in non-steady airflows.

Quite different aerosolization mechanisms take place during nebulization of liquid drugs, where aerosol droplets are typically generated by pneumatic, ultrasonic, or mesh atomization (Ari, 2014; Mitchell et al., 2023). Aerosol released from the nebulizer is transported with the additional airflow taken by the patient during normal (unforced) breathing. As the aerosol mixes with the air, the droplets can partially evaporate if the conditions are far from the dew point temperature (i.e., the air is sufficiently dry and warm). This means that the PSDs of the aerosol both *in vitro* (measured by impactor or LD) and *in vivo* (inhaled by patient) may be different than originally released from the nebulizer. Evaporation depends on the contact time of the aerosol with the air, as well as on the dilution ratio. Both parameters change over time due to the non-stationary nature of the inhalation curve. Smaller droplets evaporate faster than larger ones, according to the "diameter-square-law" (e.g., Ochowiak et al., 2022), and it means that not only the mean diameter of the aerosol is reduced, but often the finest droplets virtually disappear, leaving an ultrafine solid residue if the liquid was a solution or dispersion. These effects should be considered for different nebulizers, and they are essential to correctly define the IVIVC for drug delivery by nebulization.

This paper discusses the results of several types of experimental studies focused on the influence of airflow dynamics on the generation and transport of aerosol particles inside

and outside various inhalers. The aim of such analysis is to improve the understanding and development of IVIVC for a better link between the information gained from inhaler testing to clinically assessed lung deposition and health effects of inhaled aerosol medicine (Newman and Chan, 2020; Pirozynski and Sosnowski, 2016).

2. METHODS

2.1. DPI studies

Essential details of the materials and methods utilized in the DPI emission kinetics study have been given in our previous paper (Dorosz et al., 2021), and they are only briefly summarized below.

2.1.1. Pharmaceutical powder blend and DPI

Commercial fluticasone propionate blend with lactose (Flutixon, 125 µg of active pharmaceutical ingredient per dose; Adamed Pharma S.A., Pieńków, Poland – Batch no. 11561047) was purchased from the local pharmacy. Flutixon was aerosolized in RS01 inhaler (RS; Plastiapae Spa, Osnago LC, Italy). It is a passive DPI in which the powder exiting the rotating capsule is dispersed due to turbulent energy from inhaled airflow. Effective DPI performance requires forceful and deep inhalation. RS inhaler has low-mid resistance ($R_D = 0.055 \text{ hPa}^{0.5} \text{ min/dm}^3$, based on our own measurements).

2.1.2. Generation of non-steady flow profiles

The realistic inhalation profiles were reproduced by the high-capacity breathing simulator ASL 5000 XL (IngMar Medical, Pittsburgh, PA, USA). Two different breathing profiles (RS1 and RS2) were used to mimic *in vitro* operation of DPI inhalers. The summary of corresponding airflow conditions for two studied cases is shown in Table 1.

Table 1. Flow parameters for two studied inhalation profiles.

Profile name	Total volume of inhaled air [dm ³]	Total inhalation time t_{inh} [s]
RS1	2.344	3.41
RS2	1.689	2.0

2.1.3. Light scattering-based investigation of aerosol emission process during passive DPI performance

Fast detection of aerosol particles released from DPIs was done using light scattering-based instrument developed in collaboration with the Faculty of Physics, Warsaw University of Technology. The method allowed to detect the time of

aerosol emission with the simultaneous measuring the flow curve by anemometric mass flowmeter (TSI Inc., Shoreview, USA). Both measuring devices were connected to the oscilloscope to superimpose these two signals. The aerosol was dispersed directly into measuring flow cell by ASL 5000 XL simulator equipped with the Auxiliary Gas Exchange Cylinder (IngMar Medical, Pittsburgh, USA) to secure the interior of piston from abrasion by the inhalation powder. Quadruplicate repetitions were done to obtain mean results.

2.1.4. Laser diffraction-based analysis of aerosolization process during passive DPI performance

Evaluation of the dispersion process of the powder blend (Flutixon) in the RS DPI for two breathing profiles (1RS and 2RS) was done using LD technique (Spraytec spectrometer, Malvern Instruments, Worcestershire, UK). The device allowed to determine the volumetric PSD with the sampling rate up to 2.5 kHz for aerosols emitted from DPI mouthpiece. The unconventional application of the open-bench configuration of Spraytec spectrometer was explained in our previous work (Dorosz et al., 2021). Results were obtained in the form of bimodal volumetric PSDs with specified modes (one for the drug and the other for the carrier). The instantaneous volume concentration of particles in the aerosol cloud was also determined (%Vol) to assess the time evolution of aerosol emission. Each experiment was repeated in at least quintuplicate to obtain mean results and calculate SD. What is more, ε parameter was determined, because it indicates the importance of the unsteady term compared to the convective term at the same instant of time, when resolving the Navier-Stokes equations for the respiration process (Dorosz et al., 2016). Its values in function of process time during analyzed breathing cycle are to be evaluated according to the formula:

$$\varepsilon(t) = D_{\text{inhaler}} \frac{1}{(u(t))^2} \frac{du(t)}{dt} \quad (1)$$

where D_{inhaler} denotes the diameter of the inhaler cross-section ($D_{\text{inhaler}} = 0.011$ m) and $u(t)$ denotes the averaged axial velocity at the outlet of the DPI mouthpiece. Fluid flow Reynolds number for time-varying volumetric flow rate $Q(t)$ was calculated to estimate the temporary regime of flow profile (Dorosz et al., 2016).

2.2. Nebulizer studies

2.2.1. Droplet size distribution

A vibrating mesh nebulizer (VMN – Intec Turbo Mesh; Intec Medical, Kraków, Poland) was chosen for the study because no gas flow through the VMN is required to release the aerosol (unlike pneumatic nebulizers). This simplifies the evaluation of the effect of additional (inhaled) air mixed with the emitted aerosol on the final PSD value. Aerosol

was generated using a physiological saline solution. The flow of air mixed with the aerosol released from the mouthpiece was measured using the anemometric mass flowmeter (described earlier). The diluted aerosol was drawn through the so-called inhalation chamber of the Spraytec spectrometer described in the test procedure for the DPI. Four variants were tested: aerosol without dilution, and diluted with 10 dm³/min (L/min), 20 dm³/min, and 30 dm³/min of air drawn from the surrounding (22 ± 2°C, 40% RH). These diluting values correspond to the onset of inspiration, passing through successive phases up to the peak inspiratory flow rate (PIFR) during the tidal breathing (mean flow rate of 15 dm³/min). Two basic parameters were evaluated from the PSDs measured with LD: volumetric median diameter, Dv50 [μm], and fine particle fraction, FPF (mass fraction of particles smaller than 5 μm). All measurements were triplicated to determine the mean values and the standard deviation of the above parameters. The average values of Dv50 and FPF for the whole inhalation period t_{inh} were calculated as:

$$\bar{x} = \frac{1}{t_{\text{inh}}} \int_0^{t_{\text{inh}}} x(t) dt \quad (2)$$

where x denotes Dv50 or FPF.

2.2.2. Predicted pulmonary deposition of inhaled aerosol

Pulmonary deposition was calculated using Multi-Path Particle Dosimetry model (MPPD, ARA Inc., Albuquerque, USA) for typical parameters of tidal breathing for adults using different PSDs obtained from the studies described in Section 2.2.1. Based on the data of regional deposition efficiencies of inhaled aerosol, the benefit factor of drug inhalation, κ , was calculated:

$$\kappa = \frac{\text{DEP P}}{\text{DEP H}} \quad (3)$$

This parameter shows the ratio of the beneficial and undesired regional drug deposition efficiencies in the lungs, where DEP P denotes the deposition efficiency in the peripheral (pulmonary) lower airways associated with therapeutic effects, and DEP H denotes the deposition efficiency in the upper airways (head region), which is usually related to side effects (Pirozynski and Sosnowski, 2016).

3. RESULTS AND DISCUSSION

3.1. Powder aerosolization during emission from a passive DPI inhaler

As shown in our previous studies (Dorosz et al., 2021), the work of breathing (inhalation) is converted into kinetic energy of the air used in the system: medicinal powder – DPI. This energy is distributed over three time intervals, which is an important issue from the point of view

of optimizing the generation, transport and delivery of an aerosolized powder drug. In the first interval (from zero to a certain point), a threshold (critical) energy is obtained, beyond which it is possible to overcome the adhesion forces in the therapeutic powder and start the emission and disaggregation of the drug in the DPI-powder system. In the second time interval (from the beginning to the end of the emission), a portion of the energy – the effective energy – is obtained, which can be used in the process of fluidization and entrainment of the powder drug, and subsequent disintegration into an aerosol emitted from the DPI inhaler. This period constitutes the emission window, which was determined experimentally and is shown in Figure 1 for both inhalation profiles (RS1 and RS2). During the third interval (after the end of emission until the end of inhalation), the remaining part of the energy can only be used in the processes of transport and deposition of particles and aggregates of medicinal powder particles in the respiratory system. For this reason, a passive DPI inhaler should be characterized by a sufficiently high internal resistance, guaranteeing the use of energy in the above-mentioned processes, and not its dissipation. On the other hand, the use of a low-resistance inhaler may be associated with better dispersion of the powder at a higher flow and with higher kinetic energy, in the middle of the inhalation. However, the aerosol generated at the time of emission will have a higher velocity, and its particles will have a greater inertia and a greater ability to deposit in the upper respiratory tract. Penetration of particles in such conditions will also be hindered by the fact that the lungs are already partly filled with air and the time available for transport is shorter. To sum up, there are two competing mechanisms – effective powder dispersion to small particle sizes and unfavorable filtration of therapeutic aerosol particles in the upper respiratory tract – which have been discussed so far.

Table 2 shows the values of work of breathing attained during inhalation, and potentially (assuming no losses) trans-

ferred to the passive DPI-powder blend system in three above-mentioned time intervals. The results indicate that the threshold level of energy necessary to supply the powder was practically negligible in both studied cases. It seems that the more intensive profile RS1 may be a more appropriate flow profile for the studied inhaler, because the kinetic energy of the gas imparted during the release of the aerosol was higher. The RS tested inhaler provided a more even distribution of energy during and after emission in the RS1 profile, while for the RS2 profile, the distribution was in favor of the emission period. Therefore, for tested DPI its efficiency is clearly related to the cost of work performed by the respiratory muscles during inhalation. This is an important aspect to consider when choosing an inhalation device for a patient with impaired breathing mechanics.

Table 2. Work of breathing potentially transferred to the passive DPI-powder blend system in three time intervals: before, during and after aerosol emission process from the inhaler.

Case	Work of breathing potentially transferred to the passive DPI-powder blend system [J]		
	Before emission	During emission	After emission
Case RS1	0.0002	0.8592	1.1328
Case RS2	0.0012	1.4975	0.6707

To further analyze the influence of the inhalation dynamics on the course of aerosol generation and release processes from the passive DPI, a series of emission time moments was isolated, which included successive values of the normalized dimensionless time: normalized emission start time, 0.1, 0.2, 0.3, 0.4, 0.5 of inspiration and normalized emission end time (the extreme values for this range are respective for the given test variants RS1 and RS2). The contributions of particles in the PSD on a log-normal plot as datasets were plotted against the particle size values. The PSD was studied in a function of time, depicted in Figure 2. The shape of the PSD distribution curve underwent dynamic transfor-

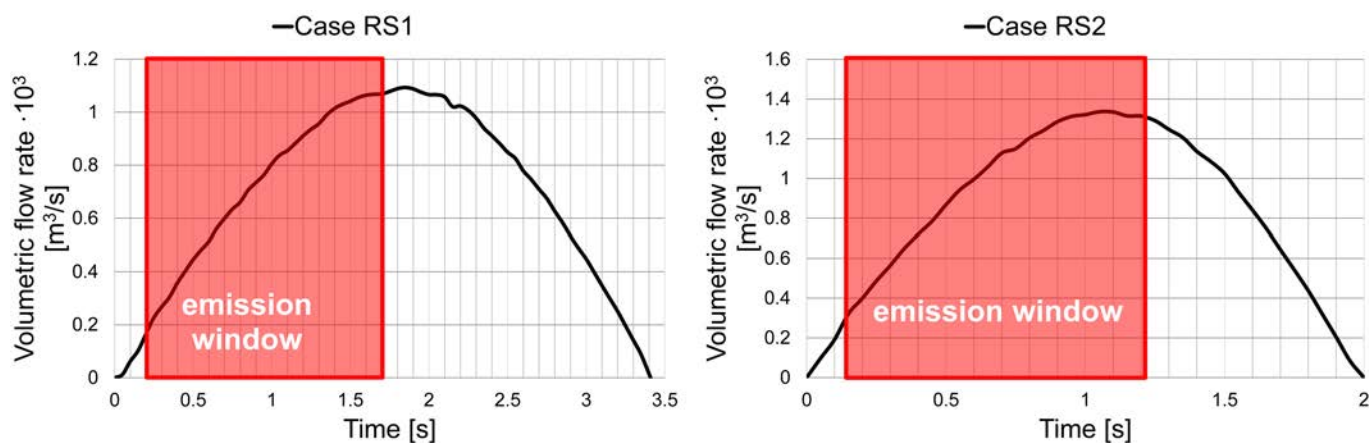


Figure 1. Experimentally determined periods of aerosol emission (emission window) for each inhalation profile (Case RS1 and RS2).

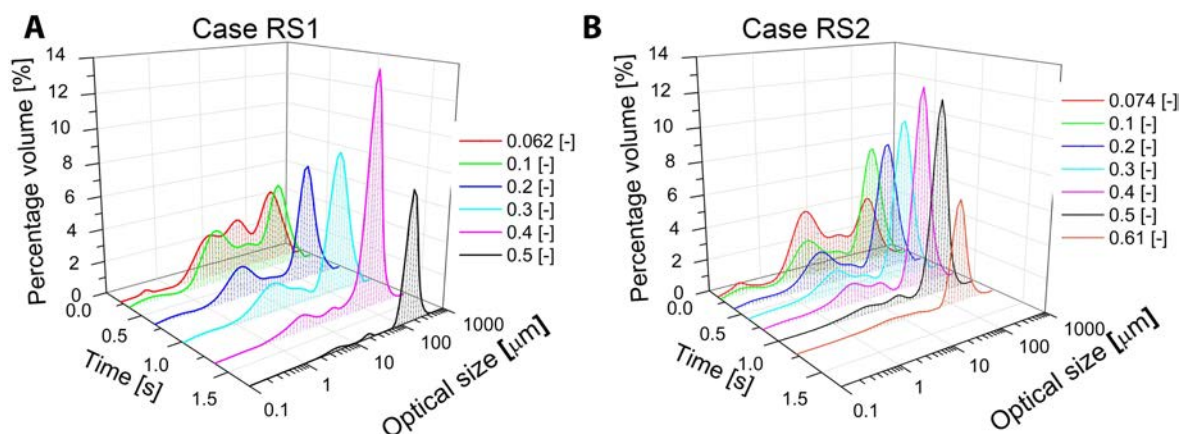


Figure 2. Time evolution of the volumetric particle size distribution for both tested flow profiles: (A) Case RS1, (B) Case RS2. Legend indicates the normalized instant of time.

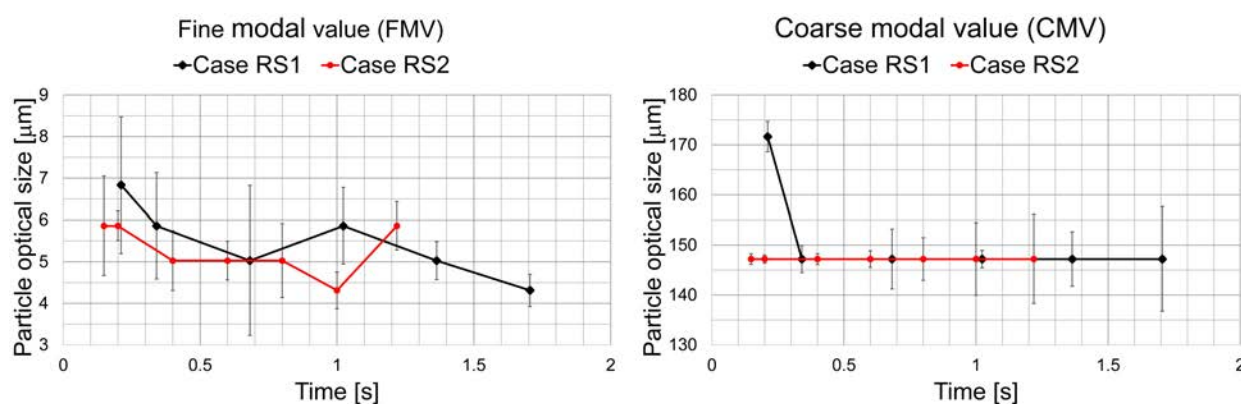


Figure 3. Fine (FMV) and coarse modal value (CMV) in time series determined based on the volumetric particle size distribution for Case RS1 and Case RS2. Error bars show the standard deviation.

mations during the aerosol emission, which proved that the aerosol cloud was reorganized in the progressing dispersion process. Two main modal values (dominants) of the distribution were distinguished, corresponding to the local maxima, which in a way identify fractions of particles of various sizes. The first dominant, marked as FMV (fine modal value), observed in the area of fine particles with a size not exceeding 10 microns and the second dominant, marked as CMV (coarse modal value), observed in the area of large particles, the size of which ranges from about one hundred to several hundred microns. As a supplement to the analysis of the time evolution of the volumetric PSD distribution of aerosol particles, the FMV and CMV modal values are additionally shown in the graphs (Figure 3) at the times indicated earlier for comparisons of results between variants RS1 and RS2. These results took the analysis deeper into understanding the aerosol dispersion behavior (the breaking up of agglomerates to regenerate the primary particles and bigger aggregates).

The dominant FMV corresponded to a range of particle sizes dispersed from 0 to approximately 10–15 μm , which can certainly be attributed to the fraction of primary API particles, as well as aggregates of API particles with fine carrier parti-

cles. Based on the graphs of dominants' variation over time, the FMV modal value oscillated around 5 μm in both analyzed RS1 and RS2 variants. The percentage share of dominant FMV in the distribution, with an initial upward trend, then gradually decreased, which was noted in all the tested variants. This was the consequence of shifting the distribution shares to the area of larger particles, which in turn resulted from the fact that dispersion occurs most effectively in the first moments of inhalation, and then the dispersion becomes weaker. In the case of the "RS" inhaler, the reduction of the fine particle mode share was from 3.4% vol. for RS1 and from 4.2% vol. for RS2. The CMV modal value represents large aggregates of particles and coarse carrier grains, occurring alone or together with smaller particles – API or carrier – deposited on its surface. The "RS" inhaler produced an aerosol characterized by a stable CMV dominant of 150 μm , only at the beginning of the analyzed inhalation curve 1 the value of the mode in one analyzed time moment was 170 μm .

Figure 4 illustrates the time evolution of two important flow parameters: Re and ε for both flow profiles (cases RS1 and RS2). At the beginning of inhalation, the regime of the flow changed from laminar to transient for both

inhalation profiles. With a further increase in the air flow rate forced through inhaler, turbulence of the flow occurred. After reaching the peak inspiratory flow rate (PIFR) which corresponds to the maximum of Re , the flow evolves into transitional and back to laminar until the end of inspiration. This type of flow regime evolution has been reported previously (Dorosz et al., 2016).

The results obtained here allow to demonstrate that aerosol release from the inhaler started when Re reached approximately 1400 (RS1) or 1500 (RS2), which corresponds to the transition from laminar to partly turbulent flow. This result is in line with the understanding of the dispersion process, which is favored by the developing turbulence of the flow in the internal channels of the inhaler. Considering the effect of non-stationarity of the inspiratory flow for uptake and de-aggregation of medicinal powder, the value of the ε parameter should be carefully monitored in real-time. At the initial moment of inhalation, ε is infinite, after which it rapidly decreases to almost zero (within approx. 2% of the total time of inhalation). The aerosol cloud emission from the inhaler was recorded when ε was equal 0.044 (RS1) or 0.026 (RS2). After that it was practically equal to zero for the remaining part of inspiration, respectively. At the end of inspiration, the course of change in the ε parameter was reversed, with a rapid decline to minus infinity in a short period before reaching zero flow. It was found that in each case studied, the moment of aerosol emission occurred shortly after crossing the time corresponding to the turning point of the ε -curve, where the function is represented by a straight line and its values are constant (close to zero). The asymptotic rate of decrease of ε is because the flow and velocity are just beginning to increase from zero, so the flow acceleration is the highest in these first moments of inhalation. Despite the low values of flow and respiratory power in this crucial period when the kinetic energy of air starts to increase from zero and the energy transfer to the inhaler-capsule with medicinal powder system begins, the non-stationarity of the fluid movement in the system plays a fundamental role in the process of excitation of the medicinal blend powder.

Then, the powder bed is fluidized and resuspended in the flow field. The results presented in Figure 4 therefore confirm the high importance of the initialization and acceleration of the airflow in the passive DPI inhaler, for the entrainment of medicinal powder and its emission as aerosol. They also indicate the limitations of typical analyses of aerosolization process with constant-flow conditions which can be a reason of poor IVIVC.

3.2. Nebulization

The studies concerning VMNs were focused on the effect of air taken in during inhalation on the actual properties of the aerosol delivered from the nebulizer. Figure 5 shows the variation of the volumetric median diameter (Dv_{50}) and the fine particle fraction (FPF) after aerosol mixing with different amounts of air. A gradual decrease of Dv_{50} and an increase of FPF are observed, and the relationships vs. airflow rate are not linear. There is a strong increase (from 25 to 35%) in FPF after dilution with the small airflow (10 dm³/min). FPF remains approximately constant for dilution with 10–20 dm³/min but increases again (to 38%) at the highest dilution corresponding to PIFR (30 dm³/min).

These results are in general agreement with the recent results of aerosol fate in the nebulizer mouthpiece obtained with CFD (Sosnowski et al., 2022). Assuming the inhalation curve (profile) at rest, $Q(t)$ can be approximated by sinus function, the airflow variation during inhalation is represented by the line shown in Figure 6. This pattern is valid for the breathing at rest (so-called tidal breathing, typically applied during nebulization), i.e., the frequency equal to 12 cycles/min and inhalation period equal to 40% of the total time of the breathing cycle ($t_{inh} = 2$ seconds) (Sosnowski et al., 2021).

Considering the above, one can calculate the changes in Dv_{50} and FPF during aerosol inhalation, based on the experimental data for selected flows (shown in Figure 6) and interpolated values of these parameters for other flows. The results of such calculations are shown in Figure 7.

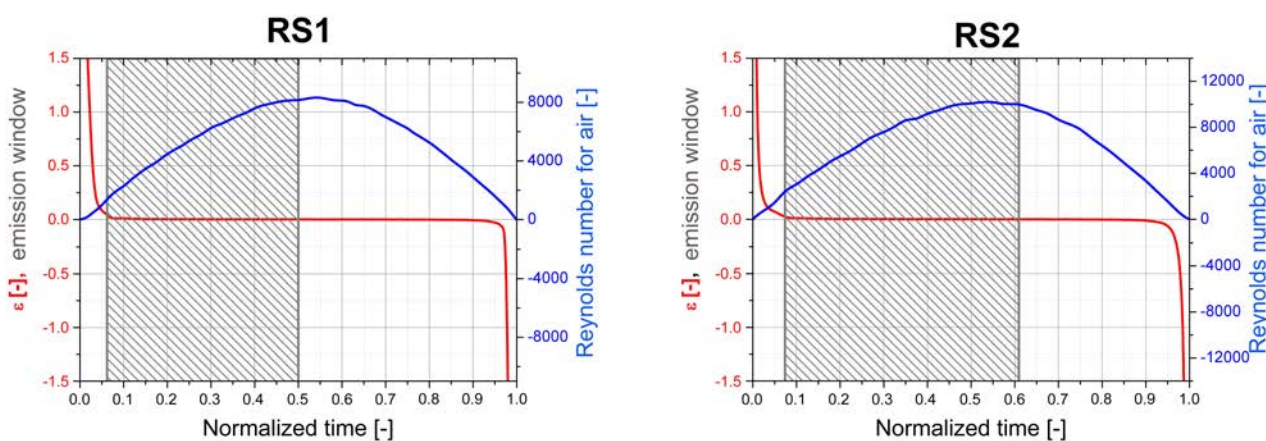


Figure 4. Fluid flow Reynolds number and ε parameter in time series for cases (profile) RS2 and RS2.

It is interesting to note that data measured at PIFR underestimate Dv_{50} and overestimate the FPF that are representative for the whole inhalation. Based on Eq. 3, the Dv_{50} and FPF values averaged across the whole inhalation period are $6.2 \mu\text{m}$ and 35.1%, respectively. These values roughly correspond to the data measured for the diluting airflow equal to 20 L/min.

Figure 8 shows a comparison of κ values calculated for aerosol Dv_{50} obtained at different dilutions. The data were obtained by calculating the predicted deposition of aerosol droplets delivered from VMN (after dilution with air) in different parts of the respiratory system (see: Eq. (4)). Again, neither the size determined at no dilution nor at PIFR can be used to correctly predict the beneficial effects of drug delivery

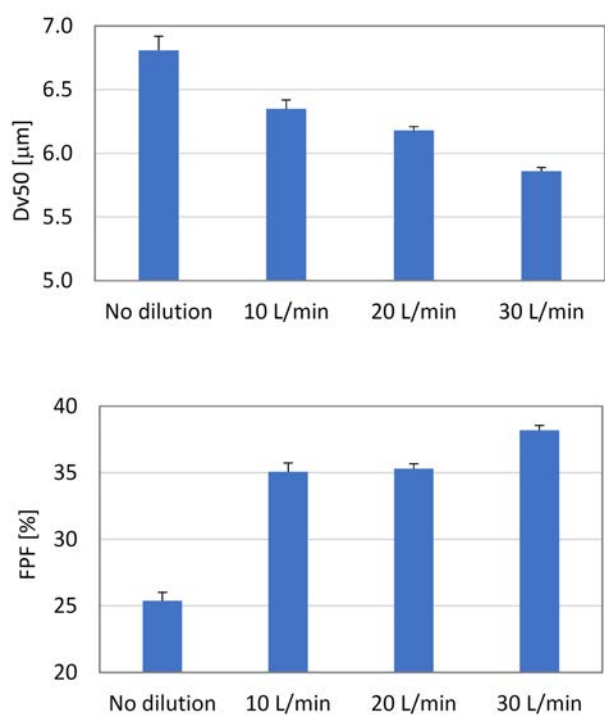


Figure 5. Change in Dv_{50} and FPF after aerosol dilution with external air ($22 \pm 2^\circ\text{C}$, 40% RH). Error bars denote standard deviation ($n = 3$).

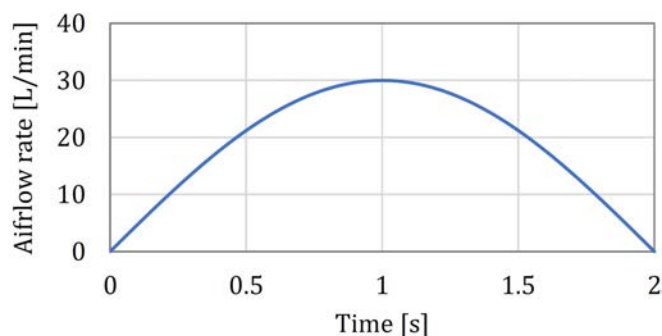


Figure 6. Airflow rate during inhalation (tidal breathing with 12 cycles/min, inhalation lasts 40% of the breathing cycle).

by inhalation. However, the κ value for the entire inhalation is close to that measured at a dilution rate of 20 L/min. Therefore, it may be suggested that using this dilution to determine the PSD in this VMN tested under typical conditions (room temperature, average humidity) should result in the best IVIVC.

4. CONCLUSIONS

The results presented in this work clearly demonstrate that airflow dynamics plays an important role in the generation and fate of aerosol particles released from different inhaling devices. In the passive DPIs, the flow intensification during the initial phase of inhalation strongly influences the time

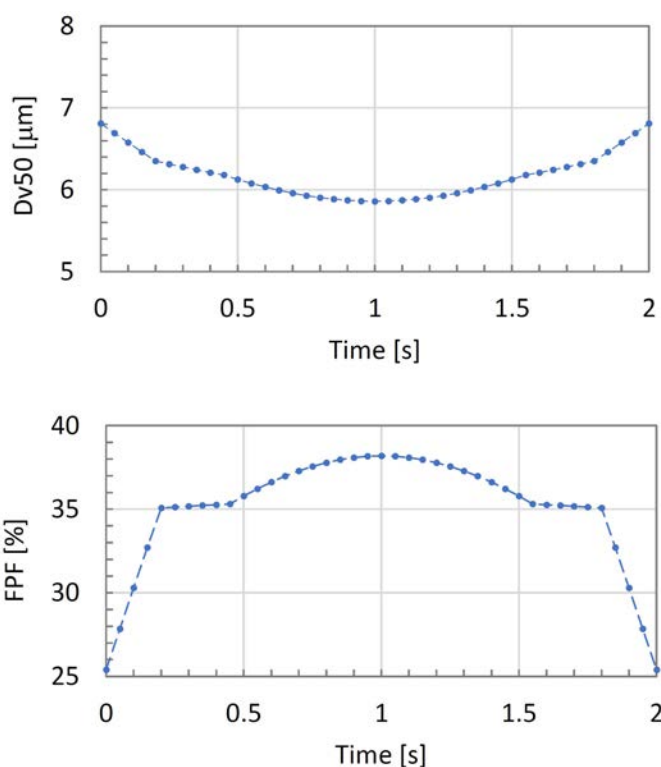


Figure 7. Temporary values of Dv_{50} and FPF during inhalation.

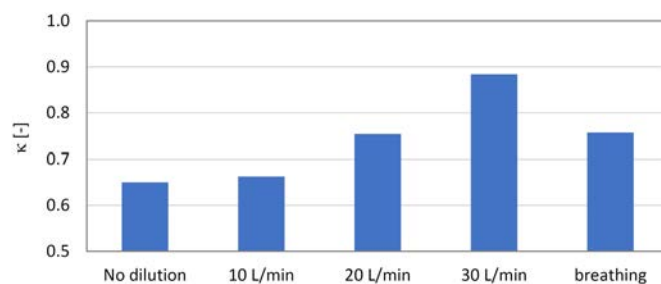


Figure 8. The benefit factor of drug inhalation κ (Eq. (3)) for different aerosol dilutions with air and realistic breathing.

evolution of particle size distribution, so in general the results obtained during measurements at constant flow are not realistic. The unsteadiness acquired from initial and relatively small values of flow rates are determinants of the energy threshold value necessary to overcome adhesion and cohesion forces within the powder blend to initiate aerosol generation and release. Another finding is that the process of aerosol emission occurs only in the first part of the inhalation process, before the peak inspiratory flow rate (PIFR) is achieved. The importance of these results for *in vitro*–*in vivo* correlation issues (IVIVC) is that in general there may be no arguments for testing DPIs at flows equal to PIFR, since no aerosol is generated nor released at such conditions (the drug has been already emitted). The presented DPI study also presents the laser diffraction method and optical detection technique of aerosol measurement in the light of their advantages when applied in *in vitro* – *in vivo* correlations (IVIVCs) and in studies using Quality by Design approach.

In the nebulization studies it was found that aerosol PSD is significantly altered due to the dilution of ambient air that is always taken in by the patient during inhalation. It follows that neither direct sampling of undiluted aerosol directly at the nebulizer mouthpiece nor measurements at high dilution (corresponding to PIFR, commonly considered as the representative flow in aerosol therapy) provide reliable information about the properties of aerosol generated and inhaled throughout inhalation. FPF values measured without dilution underestimate deposition in the lungs and consequently overestimate the side effects caused by drug deposition in the mouth and throat. This also was confirmed by the values of the benefit factor κ , which indicates the ratio of the probability of deposition in both regions of the respiratory system. Interestingly, the values measured at dilution with 20 L/min of air show the best agreement with FPF calculated as an average for the whole inhalation and with κ for real inhalation. Thus, the correct IVIVC conditions for the VMN under study can be suggested.

REFERENCES

- Ari A., 2014. Jet, ultrasonic, and mesh nebulizers: an evaluation of nebulizers for better clinical outcomes. *Eurasian J. Pulmonol.*, 16, 1–7. DOI: [10.5152/ejp.2014.00087](https://doi.org/10.5152/ejp.2014.00087).
- Azouza W., Chrystyn H., 2012. Clarifying the dilemmas about inhalation techniques for dry powder inhalers: integrating science with clinical practice. *Prim. Care Respir. J.*, 21, 208–213. DOI: [10.4104/pcrj.2012.00010](https://doi.org/10.4104/pcrj.2012.00010).
- Buttini F., Rozou S., Rossi A., Zoumpliou V., Rekkas D.M., 2018. The application of Quality by Design framework in the pharmaceutical development of dry powder inhalers. *Eur. J. Pharm. Sci.*, 113, 64–76. DOI: [10.1016/j.ejps.2017.10.042](https://doi.org/10.1016/j.ejps.2017.10.042).
- Colthorpe P., Voshaar T., Kieckbusch T., Cuoghi E., Jauernig J., 2013. Delivery characteristics of a low-resistance dry-powder inhaler used to deliver the long-acting muscarinic antagonist glycopyrronium. *J. Drug Assess.*, 2, 11–16. DOI: [10.3109/21556660.2013.766197](https://doi.org/10.3109/21556660.2013.766197).
- Corcoran T.E., Shortall B.P., Kim I.K., Meza M.P., Chigier N., 2003. Aerosol drug delivery using heliox and nebulizer reservoirs: results from an MRI-based pediatric model. *J. Aerosol Med. Pulm. Drug Delivery*, 16, 263–271. DOI: [10.1089/089426803769017631](https://doi.org/10.1089/089426803769017631).
- Delvadia R.R., Longest P. W., Byron P.R., 2012. *In vitro* tests for aerosol deposition. I: scaling a physical model of the upper airways to predict drug deposition variation in normal humans. *J. Aerosol Med. Pulm. Drug Delivery*, 25, 32–40. DOI: [10.1089/jamp.2011.0905](https://doi.org/10.1089/jamp.2011.0905).
- Delvadia R., Hindle M., Worth Longest P., Byron P. R., 2013. *In vitro* tests for aerosol deposition II: IVIVCs for different dry powder inhalers in normal adults. *J. Aerosol Med. Pulm. Drug Delivery*, 26, 138–144. DOI: [10.1089/jamp.2012.0975](https://doi.org/10.1089/jamp.2012.0975).
- Dorosz A., Penconek A., Moskal A., 2016. *In vitro* study on the aerosol emitted from the DPI inhaler under two unsteady inhalation profiles. *J. Aerosol Sci.*, 101, 104–117. DOI: [10.1016/j.jaerosci.2016.07.014](https://doi.org/10.1016/j.jaerosci.2016.07.014).
- Dorosz A., Żączek M., Moskal A., 2021. Dynamics of aerosol generation and release – dry powder inhaler performance considerations. *J. Aerosol Sci.*, 151, 105673. DOI: [10.1016/j.jaerosci.2020.105673](https://doi.org/10.1016/j.jaerosci.2020.105673).
- EDQM, 2021. Chapter 2.9.18. Preparations for inhalation: Aerodynamic assessment of fine particles, In: European Directorate for the Quality of Medicines and HealthCare (EDQM), *European Pharmacopeia. Published in accordance with the Convention on the Elaboration of a European Pharmacopoeia (European Treaty Series no. 50)*. 10th edition, Council of Europe, European Directorate for the Quality of Medicines and Health-care, Strasbourg, 347–360.
- Gac J., Sosnowski T.R., Gradoń L., 2008. Turbulent flow energy for aerosolization of powder particles. *J. Aerosol Sci.*, 39, 113–126. DOI: [10.1016/j.jaerosci.2007.10.006](https://doi.org/10.1016/j.jaerosci.2007.10.006).
- Hatley R. H. M., Byrne S. M., 2017. Variability in delivered dose and respirable delivered dose from nebulizers: are current regulatory testing guidelines sufficient to produce meaningful information? *Med. Devices: Evidence Res.*, 10, 17–28. DOI: [10.2147/MDER.S125104](https://doi.org/10.2147/MDER.S125104).
- Longest P. W., Son Y.-J., Holbrook L., Hindle M., 2013. Aerodynamic factors responsible for the deaggregation of carrier-free drug powders to form micrometer and submicrometer aerosols. *Pharm. Res.*, 30, 1608–1627. DOI: [10.1007/s11095-013-1001-z](https://doi.org/10.1007/s11095-013-1001-z).
- Marriott C., MacRitchie H.B., Zeng X.-M., Martin G.P., 2006. Development of a laser diffraction method for the determination of the particle size of aerosolized powder formulations. *Int. J. Pharm.*, 326, 39–49. DOI: [10.1016/j.ijpharm.2006.07.021](https://doi.org/10.1016/j.ijpharm.2006.07.021).
- Mitchell J.P., Carter I., Christopher J.D., Copley M., Doub W.H., Goodey A., Gruenloh C.J., Larson B.B., Lyapustina S., Patel R.B., Stein S.W., Suman J.D., 2023. Good practices for the laboratory performance testing of aqueous oral inhaled products (OIPs): an assessment from the international pharmaceutical aerosol consortium on regulation and science (IPAC-RS). *AAPS PharmSciTech*, 24, 73. DOI: [10.1208/s12249-023-02528-5](https://doi.org/10.1208/s12249-023-02528-5).
- Newman S.P., Chan H.-K., 2008. *In vitro/in vivo* comparisons in pulmonary drug delivery. *J. Aerosol Med. Pulm. Drug Delivery*, 21, 77–84. DOI: [10.1089/jamp.2007.0643](https://doi.org/10.1089/jamp.2007.0643).

- Newman S.P., Chan H.-K., 2020. *In vitro–in vivo* correlations (IVIVCs) of deposition for drugs given by oral inhalation. *Adv. Drug Delivery Rev.*, 167, 135–147. DOI: [10.1016/j.addr.2020.06.023](https://doi.org/10.1016/j.addr.2020.06.023).
- Ochowiak M., Bielecki Z., Bielecki M., Włodarczak S., Krupińska A., Matuszak M., Choiński D., Lewtak R., Pavlenko I., 2022. The D^2 -law of droplet evaporation when calculating the droplet evaporation process of liquid containing solid state catalyst particles. *Energies*, 15, 7642. DOI: [10.3390/en15207642](https://doi.org/10.3390/en15207642).
- Pirozynski M., Sosnowski T.R., 2016. Inhalation devices: from basic science to practical use, innovative vs generic products. *Expert Opin. Drug Delivery*, 13, 1559–1571. DOI: [10.1080/17425247.2016.1198774](https://doi.org/10.1080/17425247.2016.1198774).
- Shekunov B.Y., Chattopadhyay P., Tong H.H.Y., Chow A.H.L., 2007. Particle size analysis in pharmaceuticals: principles, methods and applications. *Pharm. Res.*, 24, 203–227. DOI: [10.1007/s11095-006-9146-7](https://doi.org/10.1007/s11095-006-9146-7).
- Sosnowski T.R., 2016. Selected engineering and physicochemical aspects of systemic drug delivery by inhalation. *Curr. Pharm. Des.*, 22, 2453–2462. DOI: [10.2174/1381612822666160128145644](https://doi.org/10.2174/1381612822666160128145644).
- Sosnowski T.R., 2023. Aerosols and human health – a multiscale problem. *Chem. Eng. Sci.*, 268, 118407. DOI: [10.1016/j.ces.2022.118407](https://doi.org/10.1016/j.ces.2022.118407).
- Sosnowski T.R., Janeczek K., Grzywna K., Emeryk A., 2021. Mass and volume balances of nebulization processes for the determination of the expected dose of liquid medicines delivered by inhalation. *Chem. Process Eng.*, 42, 253–261. DOI: [10.24425/cpe.2021.138929](https://doi.org/10.24425/cpe.2021.138929).
- Sosnowski T.R., Marczyk K., Dobrowolska L., Moskal A., 2022. Influence of selected parameters of nebulization process on the efficiency of targeted drug delivery to the lungs. In: B. Kawalec-Pietrenko (Ed.) *Multiphase Flows and mechanical operations of process engineering (Przepływy wielofazowe i operacje mechaniczne Inżynierii procesowej)*. Publishing House of Gdańsk University of Technology, Gdańsk, 101–106 (in Polish).
- Svensson M., Berg E., Mitchell J., Sandell D., 2018. Laboratory study comparing pharmacopeial testing of nebulizers with evaluation based on Nephele mixing inlet methodology. *AAPS PharmSciTech*, 19, 565–572. DOI: [10.1208/s12249-017-0860-8](https://doi.org/10.1208/s12249-017-0860-8).
- Telko M.J., Hickey A.J., 2005. Dry powder inhaler formulation. *Respir. Care*, 50, 1209–1227.
- United States Pharmacopeial Convention, 2021. Chapter 601 – Inhalation and nasal drug products: Aerosols, sprays and powders – performance quality tests, In: *The United States Pharmacopeia. The National Formulary. USP 44 NF 39*.
- Wei X., Hindle M., Delvadia R. R., Byron P. R., 2017. *In vitro* tests for aerosol deposition. v: using realistic testing to estimate variations in aerosol properties at the trachea. *J. Aerosol Med. Pulm. Drug Delivery*, 30, 339–348. DOI: [10.1089/jamp.2016.1349](https://doi.org/10.1089/jamp.2016.1349).
- Wei X., Hindle M., Kaviratna A., Huynh B. K., Delvadia R. R., Sandell D., Byron P. R., 2018. *In vitro* tests for aerosol deposition. VI: realistic testing with different mouth-throat models and *in vitro – in vivo* correlations for a dry powder inhaler, metered dose inhaler, and soft mist inhaler. *J. Aerosol Med. Pulm. Drug Delivery*, 31, 358–371. DOI: [10.1089/jamp.2018.1454](https://doi.org/10.1089/jamp.2018.1454).